EXPERIMENTAL AND FINITE ELEMENT MODELING OF PENETRATING TRAUMATIC BRAIN INJURY

Jiangyue Zhang, Narayan Yoganandan, Frank A. Pintar, Thomas A. Gennarelli
Department of Neurosurgery, Medical College of Wisconsin,
VA Medical Center,
Milwaukee, WI, USA

ABSTRACT

To study penetrating traumatic brain injury biomechanics, a full metal jacket 9-mm handgun projectile was discharged into a transparent brain simulant (Sylgard gel). Five pressure transducers were placed at the entry (two), exit (two), and center (one) of the simulant. High-speed digital video photography at 20,000 frames per second (fps) was used to capture the temporal cavity pulsation. Pressure histories and high-speed video images were synchronized with a common trigger. Pressure data were sampled at 308 kHz. The 9-mm projectile had an entry velocity of 378 m/s and exit velocity of 259 m/s. Kinetic energy lost during penetration was 283.7 J. The projectile created temporary cavity with maximum diameter of 54 mm. Collapsing of the temporary cavity drew the brain simulant toward the center of the cavity and created negative pressures of approximately -0.5 atmospheric pressure in the surrounding region. Pressures reached approximately +2 atmospheric pressure when temporary cavity collapsed. A three-dimensional finite element model was developed and validated with the pressure data from the experiment. The model revealed that shear deformations were pronounced in the region immediately adjacent to the projectile path (within 10 mm). Radial deformations extended further away from projectile path and widely spread through the model. These quantified data may assist in understanding injury biomechanics and management of penetration brain trauma.

Keywords: penetrating traumatic brain injury, brain simulant, physical model, finite element model, biomechanics.

Penetrating Traumatic Brain Injury (pTBI) continues to be a public health problem in the United States (CDC 2004). Firearm injuries are the second leading cause of injury-related fatalities and account for 19% of total injury-related deaths. Although treatment methods advance and duration of injury to treatment shortens, pTBI remains the most lethal injury and, therefore, warrants biomechanical studies (Gennarelli et al., 1994).

Most firearm wounding studies were performed in the military domain, using large gelatin blocks (100-150×25×25 cm) with unconstrained boundaries to capture the entire projectile path (Fackler et al., 1984; Fackler and Malinowski 1985; Fackler and Malinowski 1988). Blocks were cut open along the projectile path post testing. Permanent cavity and penetration distance were measured directly from the cut surface of the block. Maximum temporary cavity diameter was assumed by adding the radius of two of the largest radial cracks. These studies focused on quantifying projectile wounding potential. Compared to these models, human head is smaller and the brain is enclosed in the cranium. Results from these studies may not be directly applicable to pTBI studies.

Various physical models have been used to study biomechanics of civilian pTBI. In a series of recent papers, Thali et al. used a spherical head model to reproduce gunshot wounds to the head (Thali et al., 2002b). Various projectiles were used to study the creation of external gunshot wounds with high-speed photography. In a follow-up study, more human-like skull geometry was used (Thali et al., 2002a). However, these studies focused on the external wounding morphology for forensic purposes. Temporary cavities and pressures inside the model were not investigated. Yoganandan et al. compared temporary cavity dynamics of expanding and non-expanding projectiles in gelatin blocks (Yoganandan et al., 1997). Stark contrasts were found in mechanics of penetration and resulting transient and residual wound involvement between the two types of projectiles. However, no pressure data were obtained, and the applicability of this model to brain injuries was not addressed.

Injuries can occur from pressure changes accompanying passage of a projectile (Harvey et al., 1947). Watkins et al. used human dry skulls filled with 20% ordnance gelatin (Watkins et al., 1988). Steel ball bearings were used as projectiles, and pressure histories were measured at the center of the head models. Temporary cavity dynamics were sketched from 1,000 frames/second (fps) cine X-ray films. However, the frame rate was too slow to quantify the ballistic impact to the head that typically occurs in the microsecond range. Furthermore, pressure was quantified from one location. Quantification of pressures from multiple locations is necessary to better understand injury dynamics. Correlation of pressures with temporary cavity in the time domain may also assist in characterizing projectile dynamics.

In addition, all these investigations used ordnance gelatin, a muscle simulant. The dynamic moduli for ordnance gelatin are significantly higher than that for brain (Brands et al., 1999). The human brain also demonstrates increased dynamic modulus with increasing loading frequency, which the gelatin does not (Brands et al., 1999). Dow Corning Sylgard 527 A&B, a silicone dielectric gel, has been used as brain surrogate in blunt impact studies (Margulies et al., 1990; Brands et al., 2000; Ivarsson et al., 2002). Its mechanical properties are similar to brain tissues, and it also demonstrates rate sensitive properties (Brands et al., 1999; Brands et al., 2000). Limited research has been done using the Sylgard gel to determine brain deformations under blunt impact loading. Margulies et al. studied the influence of the falx cerebri on intracranial motion and deformation by using this brain surrogate in human and baboon skull models (Margulies et al., 1990). Ivarsson et al. used the same brain surrogate to study the influence of lateral ventricles and irregular skull base on brain kinematics under sagittal plane rotation acceleration (Ivarsson et al., 2002). To our knowledge, this simulant has not been used for brain injuries due to projectile penetration.

Based on the foregoing, the current research, using the brain simulant, was designed to quantify temporary cavity dynamics with high-speed digital video images and dynamic pressure changes at various locations and correlate gel disruption with pressure change due to projectile penetration in geometrically appropriate models. Experimental data were used to develop a validated finite element model (FEM) to further investigate pTBI biomechanics.

METHODS

Sylgard 527 A&B were mixed at a one-to-one ratio and poured into a Styrofoam box (size 20×15×15 cm). The gel was cured at room temperature for 24 hours. A layer of flexible, neutral density reference lines was embedded 2 cm apart in the vertical mid-plane of the block to describe the motion of the gel. Five pressure transducers (EPS-B01-5KP, Entran, Fairfield, NJ) were inserted into the gel block through predrilled holes in the box. One pressure transducer (Ch5) was at the center of the block and the other four were 75 mm away from Ch5 along the diagonal of the block (Fig. 1). Transducers were inserted 2.5 cm into the gelatin block, 5 cm away from the mid-plane of the gel block. The civilian projectile (9-mm) was discharged using commercially available handgun at one meter from the surface of the block. The projectile penetrated horizontally through the gel block, shown by the dotted line in figure 1. The height of the projectile path was at the level of the center pressure transducer (Ch5), with two pressure transducers (Ch4 and Ch1) above and two transducers (Ch2 and Ch3) below its path. Pressure-time history data were collected at a sampling rate of 308 kHz using a digital data acquisition system (TDAS Pro, DTS, Inc., Seal Beach, CA) and filtered with a 5-kHz low-pass filter. High-speed digital video camera (MotionXtra HG-100k, Redlake, San Diego, CA) was used to capture the dynamic pulsation of temporary cavities. The camera was set perpendicular to the projectile path and one meter away from the outer surface of the model. The setting of the camera was at 20,000 fps and 256×192 pixels resolution. A common trigger system synchronized the high-speed video and digital data acquisition system. High-speed video images were analyzed on a frame-by-frame basis. Length (along the projectile path) and width (orthogonal to the path of the projectile) of temporary cavities were determined on each frame from one edge of the temporary cavity to the other. Times correlating pressure data and pulsation of temporary cavities, determined by size changes from video images, were analyzed. Analysis was carried out for several dynamic pulsation cycles and extended up to 12 ms, well beyond the projectile exit.

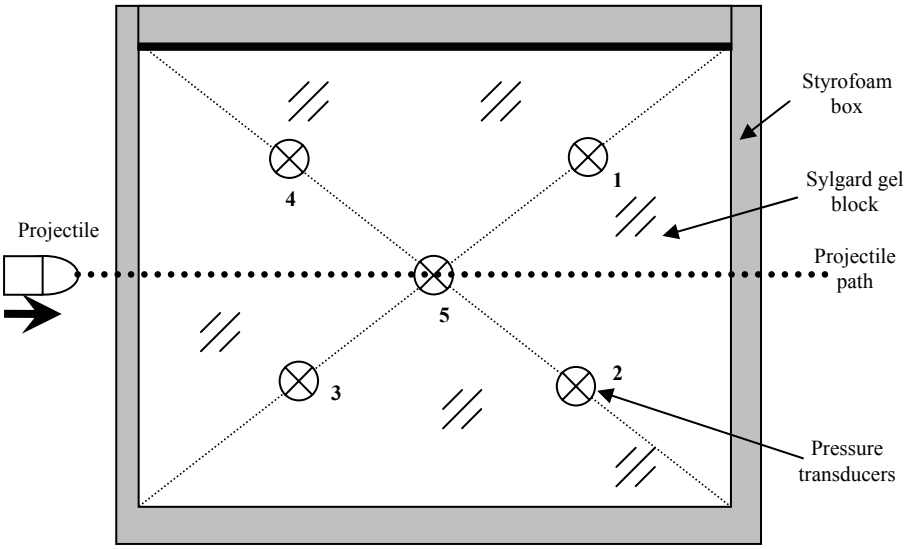

Fig. 1 – Side view of experiment setup showing the gel block. Four pressure transducers (1, 2, 3, 4) were located along the diagonal of the gel block, 75 mm from the fifth transducer placed at the center (5)

To further study the internal biomechanics in the physical model, a three-dimensional finite element model (FEM) was developed (Fig. 2) to simulate the experiment using nonlinear dynamic solver LS-DYNA (LSTC, Livermore, CA). A recently implemented hybrid Lagrangian/Eulerian method was used. In the hybrid model, the container and projectile were simulated using the Lagrangian algorithm, and the Sylgard gel was simulated using the Eulerian alogrithm. In the Lagrangian domain, the model consisted of 1,152 elements for the projectile and 25,960 elements for the container. In the Eulerian domain, the model consisted of 40,960 elements for the Sylgard gel. An extra 61,280 void Euler elements surrounding the Sylgard block were used to allow material flow within the Euler domain. An initial velocity of 378 m/s was assigned to the projectile. The bottom of the container was restricted in –Z motion, simulating the boundary condition of the model sitting on a rigid surface. Impact of projectile to gel and interaction between the gel and container were simulated using fluid-to-solid coupling. Pressures histories at locations of embedded pressure transducers were exported to validate with the experiments. Pressure and velocity distribution at the vertical mid-plane along the projectile path were studied.

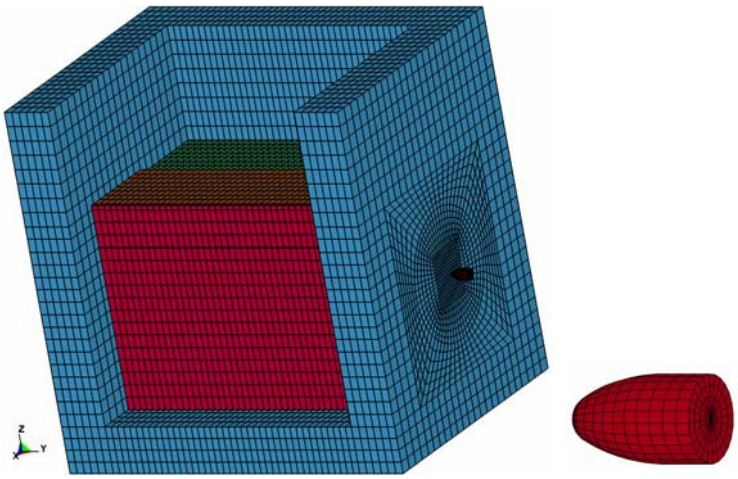

Fig. 2 – Overview of the finite element model with an enlarged projectile

RESULTS

The 9-mm projectile with an entry velocity of 378 m/s, left the gel block at 259 m/s at 0.65 ms and lost 32% velocity and 283.7 J kinetic energy. Figure 3 illustrates the high-speed video images showing the projectile penetrating process and temporary cavity pulsation after projectile exit.

During the penetrating process, projectile dragged the gel forward and pushed the gel away from its path, creating a temporary cavity along its path. Tips of torn reference lines pointed forward in the direction of the projectile and kinked at contact with the cavity. The initial cavity appeared conical in shape with the larger end toward projectile entry and affected reference lines only in the immediate region defined by the temporary cavity (Fig. 3a-c). Reference lines away from temporary cavities maintained their initial position during and immediately after the time at which the projectile was traveling in the gel block. After projectile exit, the cavity diameter continued to expand, while the cavity length remained the same (Fig. 4). The maximum cavity (Fig. 3d, at 2.5 ms, length: 180 mm, diameter: 54 mm) appeared cylindrical with a larger diameter toward the exit. The cavity collapsed and expanded freely after the maximum cavity (Fig. 3e-g). During the collapsing/expanding process of the cavity, gel was drawn toward/pushed away from the center of the block. Cavities expanded and collapsed in subsequent cycles with gradually decreasing size (Fig. 3f, 3g). Cavities appeared circular in shape during these later stages. More severe distortion occurred during the free pulsation stage, and reference lines throughout the block were distorted.

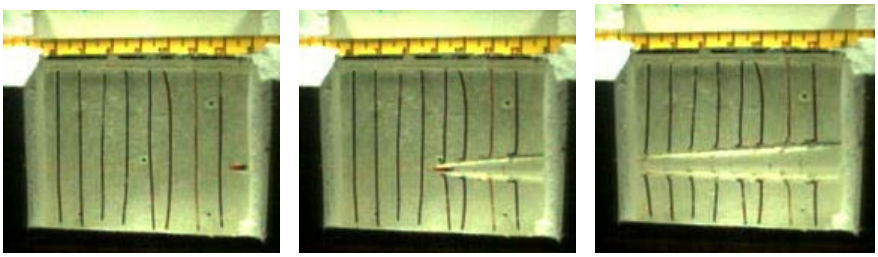

3a. 0 ms, projectile entry **3b.** 0.30 ms at the center **3c.** 0.65 ms projectile exit

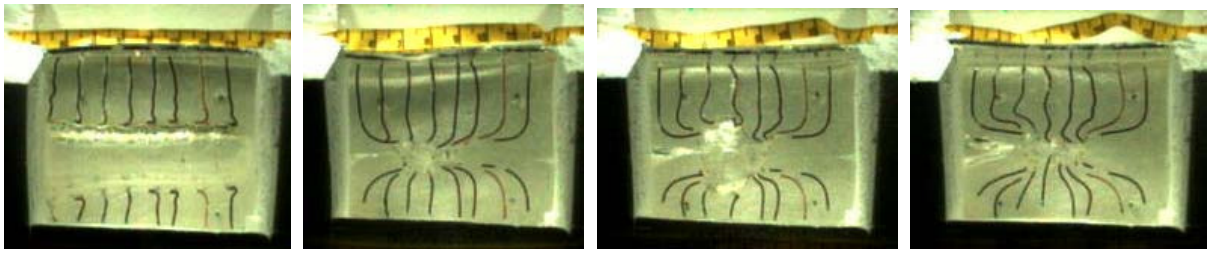

3d. 2.50 ms 1st max cavity **3e.** 6.50 ms 1st min cavity **3f.** 8.60 ms 2nd max cavity **3g.** 11.75 ms 2nd min cavity

Fig. 3 – High-speed video images of projectile penetrating process. Vertical lines were neutral density reference lines embedded in the mid-plane of the gel block

Vertical dotted lines in pressure-time history graphs (Fig. 5) correspond to time of the critical frames shown in figure 3, i.e., projectile entry, projectile exit; first and second cycle of maximum and minimum temporary cavity. Three peak high pressures were recorded by the transducer located at the center of the block. The first peak occurred during projectile penetration. The second and third peaks were associated with temporary cavity collapse. Peak pressures were 228, 242.6, and 89 kPa. Negative pressures were recorded at the middle of the first expansion and first collapse and the second expansion and second collapse. Pressure amplitudes were -52 and -30 kPa.

Pressure sensors Ch4 and Ch3 were located closer to the entry site, Ch4 above and Ch3 below the projectile path. These channels showed similar trends in peak pressures. The first peak pressures occurred immediately after the projectile entered the block. Peak pressures of 119 kPa and 106 kPa were recorded in Ch3 and Ch4 at 0.16 ms. Peak negative pressures were -45 kPa at 6.30 ms in Ch3

and -43 kPa at 2.30 ms in Ch4. Pressure sensors Ch1 and Ch2 were located closer to the exit site, Ch1 above and Ch2 below the projectile path. Peak pressure was 68 kPa at 6.50 ms, and peak negative pressure was 53 kPa at 3.90 ms in Ch1. In Ch2, peak pressure was 75 kPa at 0.50 ms, and peak negative pressure was 86 kPa at 5.90 ms.

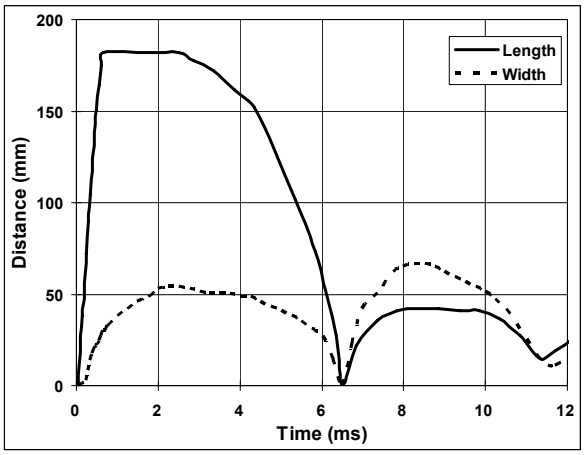

Fig. 4 – Length and width of temporary cavity

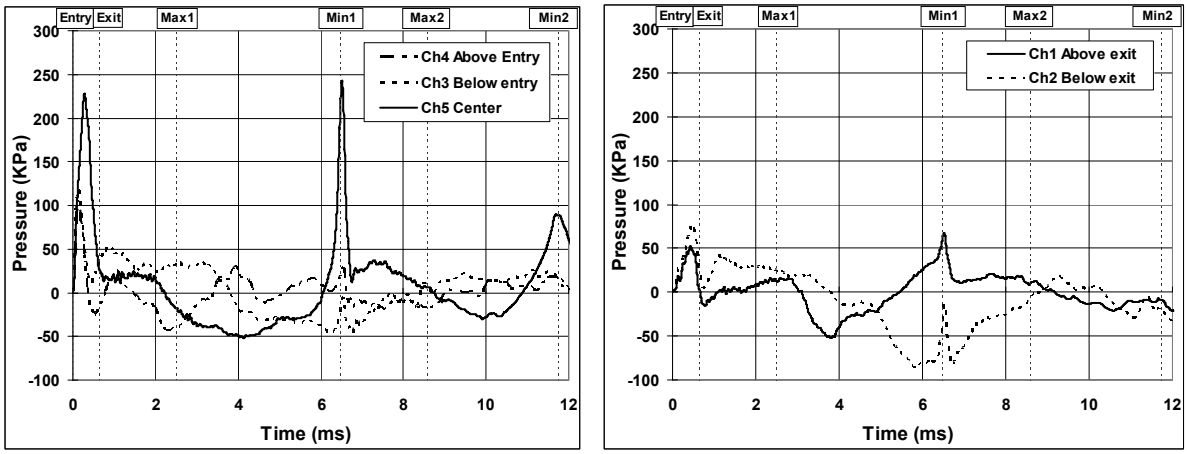

Fig. 5 – Pressure history from five channels in the model

The FEM simulating the experiment was executed until projectile exit. Pressure history at a location corresponding to the center channel pressure transducer was compared to experimental data before and after 5 kHz filter (Fig. 6). Before 5 kHz filtering, the FEM yielded peak positive pressure of 587 kPa, and experiment yielded peak positive pressure of 509 kPa. Both pressure histories oscillated at approximately 10 kHz, but amplitude of oscillation in the FEM decreased at a faster rate than the experiment. After 5 kHz filter, peak pressure was 226 kPa in experiment and 176 kPa in the FEM, and pressure pulse durations were approximately 0.7 ms in both cases.

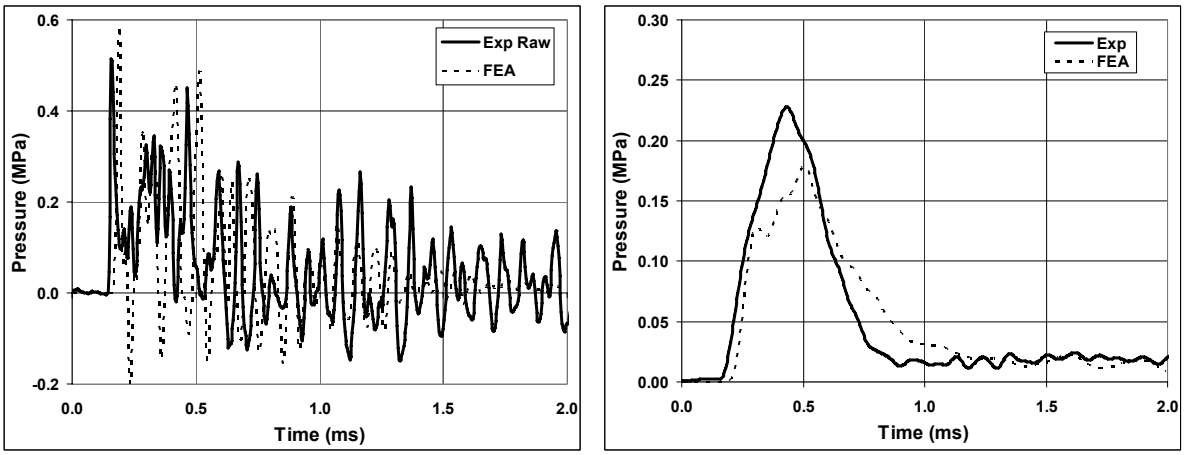

Before filter

After 5 kHz filter

Fig. 6 – Comparing of pressure history from finite element model (FEA) with experiment (Exp) at the center channel (Ch5) before and after 5 kHz filter

Pressure wave effect was significant in the initial penetration (Fig. 7a-d). Positive pressure (red area) was generated in the gel ahead of the projectile as it started penetrating (Fig. 7a). The pressure wave traveled at a speed faster than the projectile. As the projectile penetrated further, a negative pressure region (blue area) was generated behind the positive pressure front, followed by a second positive pressure wave (Fig. 7b). The first positive pressure wave front reflected from the boundary, interacted with the incoming pressure wave generating a large region of negative pressure (Fig. 7c). The wave effect continued, but as the projectile penetrated further, the wave effect damped. Pressures were mostly confined to the front of the projectile after the projectile passed the mid-point of the model (Fig. 7e-f).

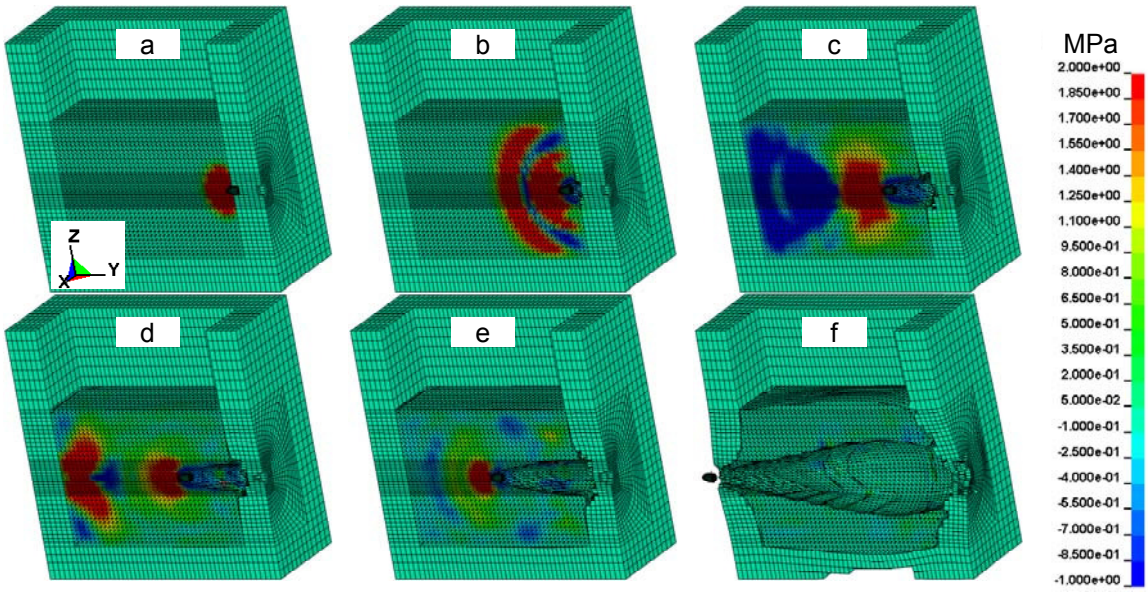

Fig. 7 – Pressure contour at the mid-plane of the block model

Velocity contour at the mid-plane of the model showed that the Sylgard gel was pushed forward and away from projectile (Fig. 8). The forward motion (velocities along the projectile path, Y direction) was confined in the immediate region less than 10 mm from projectile and immediately decreased to zero in the outer regions (Fig. 8 upper row). Gel at the entry site was pushed backward (+Y velocity, red in Fig. 8 upper row), pushing the container outward, creating a back splashing effect. The radial motion (velocities perpendicular to the projectile path, Z direction, Fig. 8 lower row) decreased linearly and extended all across the cross section of the model.

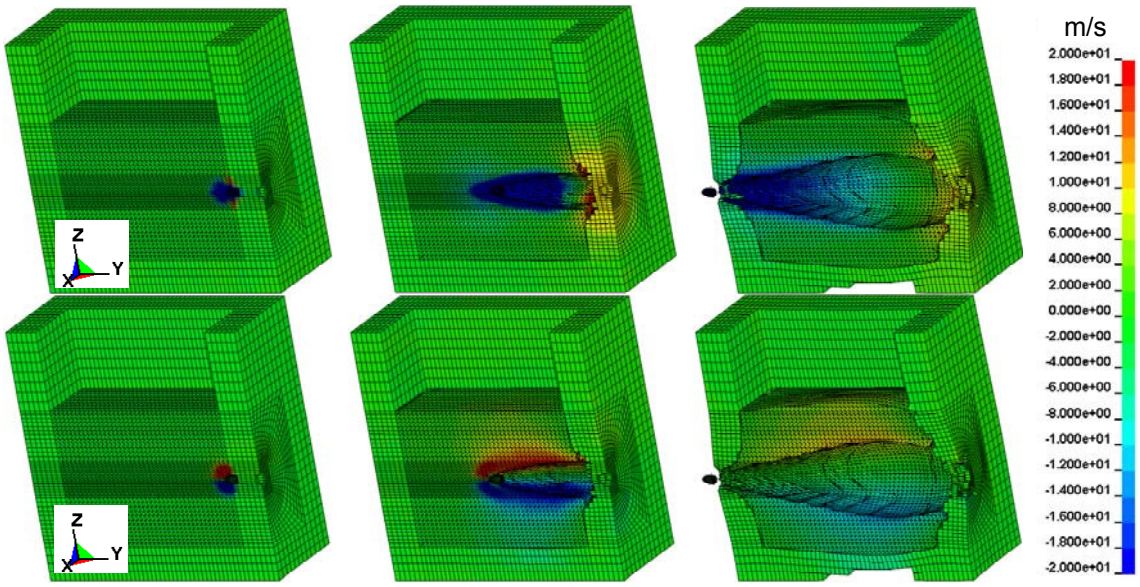

Fig. 8 – Y-velocity (upper row) and Z-velocity (lower row) contour at the mid-plane of the model

DISCUSSION

Various materials have been used to study wound ballistic effects, and ordnance gelatin is the most commonly adopted soft tissue simulant because it is translucent and has the ability to simulate muscle response to ballistic impact (Fackler and Malinowski 1985; Fackler and Malinowski 1988; Fackler 2001). In contrast, the present study used Sylgard gel because of its emphasis as a brain tissue simulant. The density of this silicon-based dielectric gel (0.975 g/cm^3) closely approximates human brain density (1.03 g/cm^3). It also demonstrates similar rate sensitive dynamic mechanical properties as the brain (Brands et al., 2000; Brands et al., 1999). Researchers have used this simulant as a brain surrogate under low-velocity blunt head-impact studies (Ivarsson et al., 2002; Margulies et al., 1990). The inherent assumption is that this simulant mimics human brain response under high-velocity projectile-induced penetrating impacts.

A small gel block (20×15×15 cm) was used in the current study. Compared to free boundary large gelatin blocks used in previous ballistic studies, the size of the gel block is a good representation of the human head (head anterior to posterior, approximately 20 cm; head breadth, approximately 15 cm). The Styrofoam container also provided a boundary to the gel similar to the boundary effect of human skull to the brain. Despite these improvements, it would be necessary to refine the geometry and boundary condition to more appropriately mimic the human head. This is a limitation of the present study.

In the current study, a hybrid Langrangian/Eulerian approach was used. The projectile and the container were modeled using the Lagrangian algorithm, and the Sylgard gel was modeled using the Eulerian algorithm. The Eulerian algorithm for the Sylgard gel allowed large local deformation for the gel (flow within the Eulerian mesh domain, creating new surfaces as the projectile penetrates). In the mean time, the material interface was maintained because the projectile and container were modeled in the Lagrangian domain. Pressure histories from the FEM matched reasonably well with experimental data before and after data filtering (Fig. 6). Sonic pressure wave reflections were found most significant in the initial penetrating stage (Fig. 7a-d). Compared to the experiment, the pressure oscillation in the FEM damped much faster. This may be due to the artificial bulk viscosity introduced in the model to stabilize the computation. For the size of the block used in the present study, the travel time of pressure wave (approximately 1,500 m/s) from one side to the other approximately 0.1 ms, i.e., 10 kHz in frequency. Similar high-frequency pressures were also reported in studies with gelatin blocks (Watkins et al., 1988).

A 5 kHz low-pass filtering was applied to the pressure history to separate pressure changes of sonic pressure wave reflection from the slow pulsation of gel movements. Figure 9 illustrates amplitude changes due to this filtering process, effects being most pronounced within the first 4 ms. Low-pass 5 kHz filtering permitted clearer appreciation of the pressure introduced by the slow pulsation of the temporary cavity. The choice of a low-pass 5 kHz filter was based on literature (Watkins et al., 1988), the fact that sonic wave pressure was at 10 kHz frequency, and pulsation of temporary cavity had a frequency of less than 300 Hz.

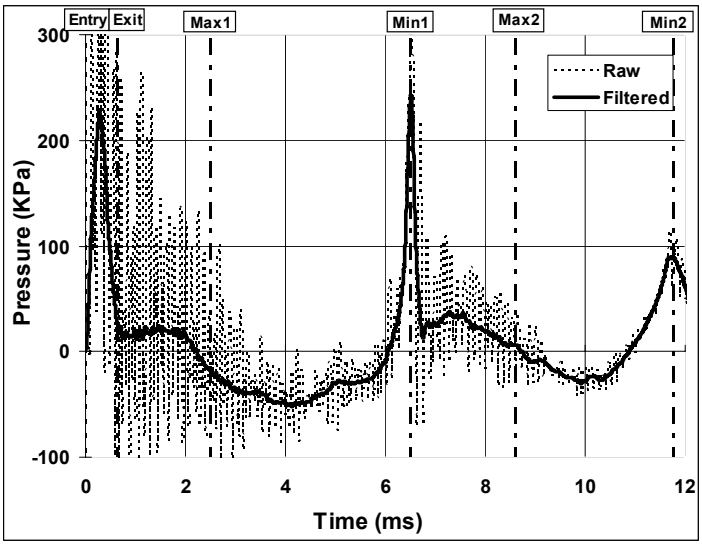

Fig. 9 – Pressure history unfiltered and 5 kHz filtered data at the center of the block

In the experiment, the first peak pressure in all channels occurred when the projectile passed in front of the respective pressure sensor. Pressure changes in the center channel (Ch5) following the projectile exit correlated with the pulsation of the temporary cavity. Peak positive pressures occurred when the temporary cavities collapsed. Peak negative pressures occurred at the interval between maximum expansion of the temporary cavity and its collapse (Fig. 5). These central pressure history patterns, i.e., first high-peak pressure corresponding to entry of the projectile followed by pressure changes due to pulsation of the temporary cavity, agreed well with literature. (Harvey et al., 1947). This previous study reported positive pressures of 414 kPa, 145 kPa, and 48 kPa when the temporary cavity volume was at a minimum with negative pressures of 103 kPa between the positive peaks.

Pressure histories in the FEM had similar shape and duration as the experimental data after 5 kHz filtering. However, the peak amplitude was lower compared to the experiment. The material property used for the Sylgard gel maybe a factor. In the Eulerian approach, an equation of state is required for the Sylgard gel. Gruneisen equation of state data for water was used as this data is not available for Sylgard gel. The higher rigid and viscosity of the Sylgard gel may have contributed to the higher pressures in experiments. Pressure contours at the mid-plane of the model found large areas of negative pressure that were created from the wave reflections from the boundary (Fig. 7c). High-amplitude negative pressure has the physical possibility of causing cavitation effects in brain tissue (Nusholtz et al., 1995). The reflected negative pressure may explain injury mechanism differences between entry and exit wounds.

Velocity contours at the mid-surface of the model showed shearing motion of the gel was concentrated in the immediate region of the projectile path (Fig. 8). It is also observed that during the initial penetration stage, reference lines were only deformed in the immediate regions to the cavity. Radial motions created tension in the annular direction, and decreased more linearly and extended all

the way to the boundary of the gel. These findings suggest that shearing injury is local to projectile path, and annular tissue tensile injury from radial displacement can spread further away from the projectile path.

To the best of our knowledge, this is the first study to use Sylgard gel as a brain surrogate rather than relying upon conventional gelatin simulants. Including the use of pressure transducers, synchronized temporary cavity formation, collapse with pressure signals, and a hybrid Euler/Lagrangian algorithm, this study evaluated the potential effects of localized pressures and their gradients on a quantitative temporal basis.

ACKNOWLEDGMENTS

This study was supported by PHS R49CCR519614 and VA Medical Research. We acknowledge the technical assistance of Reg H. Templin of the State of Wisconsin Crime Laboratory, Milwaukee, Wisconsin.

REFERENCES

Brands, D. W. A., Bovendeerd, P. H. M., Peters, G. W. M. and Wismans, J. S. H. M. The large shear strain dynamic behaviour of in-vitro porcine brain tissue and silicone gel model material. 44th Stapp Car Crash Conference, (2000).

Brands, D. W. A., Bovendeerd, P. H. M., Peters, G. W. M., Wismans, J. S. H. M., Paas, M. H. J. W. and Bree, J. L. M. J. Comparison of the dynamic behaviour of brain tissue and two model materials. 43rd Stapp Car Crash Conference, (1999) San Diego, California.

CDC. "Deaths: Injuries, 2001." National Vital Statistics Reports **52**(21): (2004) 1-87.

Fackler, M. L. "What's wrong with the wound ballistic literature and why." Wound ballistic review: Journal of the International Wound Ballistic Association **5**(1): (2001) 37-46.

Fackler, M. L. and Malinowski, J. A. "The wound profile: a visual method for quantifying gunshot wound components." J Trauma **25**(6): (1985) 522-9.

Fackler, M. L. and Malinowski, J. A. "Ordnance gelatin for ballistic studies." The American Journal of Forensic Medicine and Pathology **9**(3): (1988) 218-219.

Fackler, M. L., Surinchak, J. S. and Malinowski, J. A. "Wounding potential of the Russian AK-47 assault rifle." The Journal of Trauma: Injury, Infection, and Critical Care **24**: (1984) 263-266.

Gennarelli, T. A., Champion, H. R., Copes, W. S. and Sacco, W. J. "Comparison of mortality, morbidity and severity of 59,713 head injured pateints wiht 114,447 patiens with extracranial injuries." The Journal of Trauma: Injury, Infection, and Critical Care **37**(6): (1994) 962-968.

Harvey, E. N., Korr, I. M. and Oster, G. "Secondary damage in wounding due to pressure changes accompanying the passage of high velocity missiles." Surgery **21**: (1947) 218-239.

Ivarsson, J., Viano, D. C. and Lovsund, P. "Influence of the lateral ventricles and irregular skull base on brain kinematics due to sagittal plane head rotation." Journal of Biomechanical Engineering **124**: (2002) 422-431.

Margulies, S. S., Thibault, L. E. and Gennarelli, T. A. "Physical model simulations of brain injury in the primate." Journal of Biomechanics **23**(8): (1990) 823-836.

Nusholtz, G. S., Wylie, B. and Glascoe, L. G. "Cavitation/boundary effects in a simple head impact model." Aviat Space Environ Med **66**(7): (1995) 661-7.

Thali, M. J., Kneubuehl, B. P., Vock, P., Allmen, G. v. and Dirnhofer, R. "High-speed documented experimental gunshot to a skull-brain model and radiologic virtal autopsy." Am J Forensic Med Pathol **23**(3): (2002a) 223-228.

Thali, M. J., Kneubuehl, B. P., Zollinger, U. and Dirnhofer, R. "The "Skin-skull-brain model": a new instrument for the study of gunshot effects." Forensic Sci Int **125**: (2002b) 178-189.

Watkins, F. P., Pearce, B. P. and Stainer, M. C. "Physical effects of the penetration of head simulants by steel spheres." The Journal of Trauma: Injury, Infection, and Critical Care **28**(Supplement 1): (1988) 40-54.

Yoganandan, N., Pintar, F. A., Kumaresan, S., Maiman, D. J. and Hargarten, S. W. "Dynamic analysis of penetrating trauma." The Journal of Trauma: Injury, Infection, and Critical Care **42**(2): (1997) 266-272.